Inhibition Studies of Soybean and Human 15-Lipoxygenases with Long-Chain Alkenyl Sulfate Substrates†

Rakesh Mogul‡ and Theodore R. Holman*

Department of Chemistry and Biochemistry, University of California, Santa Cruz, California 95064

Received November 8, 2000; Revised Manuscript Received January 18, 2001

ABSTRACT: Lipoxygenases are currently potential targets for therapies against asthma, artherosceloris, and cancer. Recently, inhibition studies on both soybean (SLO) and human lipoxygenase (15-HLO) revealed the presence of an allosteric site that binds both substrate, linoleic acid, and inhibitors; oleic acid (OA) and oleyl sulfate (OS). OS ($K_D \approx 0.6$ μM) is a ≈30-fold more potent inhibitor than OA ($K_D \approx 20$ μM) due to the increased ionic strength of the sulfate moiety. To further investigate the role of the sulfate moiety on lipoxygenase function, SLO and 15-HLO were assayed against several fatty sulfate substrates (linoleyl sulfate (LS), *cis*-11,14-eicosadienoyl sulfate, and arachidonyl sulfate). The results demonstrate that SLO catalyzes all three fatty sulfate substrates and is not inhibited, indicating a binding selectivity of LS for the catalytic site and OS for the allosteric site. The 15-HLO, however, manifests parabolic inhibition kinetics with increasing substrate concentration, and it is irreversibly inhibited by these fatty sulfate substrates at high concentrations. The inhibition can be stopped, however, by the addition of detergent to the fatty sulfate mixture prior to the addition of 15-HLO. These results, combined with the modeling of the kinetic data, indicate that the inhibition of 15-HLO is due to a substrate aggregate. These substrate aggregates, however, do not inhibit SLO and could present a novel mode of inhibition for 15-HLO.

Inhibition of lipoxygenase is a significant area of research due to its implications in cancer and a variety of inflammatory diseases (*1*−*5*). Lipoxygenase catalyzes the oxidation of fatty acids using a non-heme iron center (*6*). The generally accepted mechanism for lipoxygenase involves a hydrogen atom abstraction at C-3 of the 1,4-diene by Fe(III) with subsequent trapping of the pentadienyl radical by oxygen, forming the hydroperoxide product (*7*−*11*). The microscopic rate constants of catalysis can be affected through the binding of either an inhibitor or a substrate to an allosteric site on soybean lipoxygenase[1] (SLO) and human 15-lipoxygenase (15-HLO), as demonstrated by saturation-inhibition kinetics and kinetic isotope effect (KIE) studies (*12*−*15*). A key aspect of this discovery was the conversion of oleic acid (OA) to oleyl sulfate (OS) which increased its binding affinity to the allosteric site by ≈ 30-fold ($K_i \approx 0.6$ μM for OS and ≈ 20 μM for OA) (*13*). An allosteric site was also observed on 5-HLO, through photo-cross-linking studies (*16*), suggesting that the allosteric site may be a common motif in the lipoxygenase family.

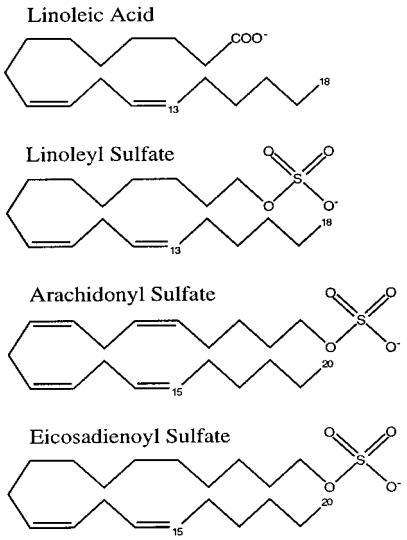

FIGURE 1: Chemical structures of fatty sulfate substrates.

In the current study, we extend our investigation of the effects of fatty sulfates (long-chain alkenyl sulfates) on the kinetic function and allosteric inhibition of SLO and 15-HLO by comparing the catalytic and inhibitory properties of several fatty sulfate substrates (linoleyl sulfate (LS), *cis*-11,14-eicosadienoyl sulfate (diES), and arachidonyl sulfate (AS), Figure 1). These data indicate that the fatty sulfates are excellent substrates for SLO but are not inhibitors, which suggests no binding to the allosteric site (*17*). The 15-HLO, however, demonstrates unusual kinetics which reveal the fatty sulfates to be substrates at low concentration (<15 μM) and irreversible inhibitors at high concentration (>20 μM). These data cannot be modeled with simple monomer inhibition and

† This work was supported by Grant GM56062-01 (NIH).

* To whom correspondence should be addressed. Phone: 831-459-5884. Fax: 831-459-2935. E-mail: tholman@chemistry.ucsc.edu.

‡ Current address: Department of Chemistry, California State University, Chico, CA 95929-0210.

[1] Abbreviations: SLO, soybean lipoxygenase-1; 15-HLO, human reticulocyte 15-lipoxygenase; LA, linoleic acid; AA, arachidonic acid; OA, oleic acid; FA, fatty acid; fatty sulfate, long-chain alkenyl sulfate; OS, oleyl sulfate or (*Z*)-9-octadecenyl sulfate; LS, linoleyl sulfate; diES, *cis*-11,14-eicosadienoyl sulfate; AS, arachidonyl sulfate; 13-HPOD, 13-hydroperoxy-9,11-(*Z*,*E*)-octadecadienoic acid; RDS, rate determining step; EI-MS, electron ionization mass spectroscopy; ICP-MS, inductively coupled plasma mass spectroscopy; KIE, kinetic isotope effect; NMR, nuclear magnetic resonance; cmc, critical micelle concentration; SDS, sodium dodecyl sulfate.

10.1021/bi002581a CCC: $20.00
Published on Web 03/16/2001

suggest the presence of substrate aggregates that irreversibly inhibit 15-HLO, by surface denaturation and/or covalent modification.

MATERIAL AND METHODS

Materials. SLO and 15-HLO were expressed and purified as described previously (*18*). Iron contents of all lipoxygenase enzymes were determined on a Finnegan inductively coupled plasma mass spectrometer (ICP-MS), using internal standards of cobalt-EDTA, and data were compared with those from standardized iron solutions. All kinetic measurements were standardized to iron content.

Fatty Acid Synthesis. Linoleyl sulfate (LS), arachidonyl sulfate (AS), and *cis*-11,14-eicosadienoyl sulfate (diES) were prepared as described previously, with the following modification (*13, 17*). After synthesis, the fatty sulfates were purified by flash silica column chromatography. The fatty sulfate (1 g) was loaded onto a 20 g silica column, washed with 3 volumes of ethyl acetate to remove the fatty alcohol, and eluted with 50:50 ethyl acetate/ethanol. The resultant material was crystallized and used for kinetics measurements.

Surface Tension Measurements. The buffers used correspond to those used in the kinetics measurements. Surface tension was measured as described by Mogul et al., using a thin platinum plate (perimeter 2.5 cm) and a Cahn electromicrobalance (*13*). The critical micelle concentrations (cmc) of all substrates (LA, LS, AS, and diES) were determined, as described previously (*13, 19*).

Substrate Kinetics. Lipoxygenase rates were determined following the formation of product at 234 nm ($\epsilon = 25\,000$ M^{-1} cm^{-1}) with a Hewlett-Packard 8453 and/or a Perkin-Elmer Lambda 40 spectrophotometer. All reactions were 2 mL in volume, run at room temperature (≈22 °C), and constantly stirred with a rotating magnetic bar. The substrate solutions used in each experiment were measured for accurate LA, LS, AS, or diES concentration by quantitatively converting substrate to product using lipoxygenase. The ϵ for all of these products is assumed to be 25 000 M^{-1} cm^{-1}. Steady-state kinetics measurements for SLO were performed in 10 mM CHES (pH 9.2) or 25 mM HEPES (pH 7.5), as indicated. Substrate inhibition kinetics measurements for 15-HLO were run in 10 or 25 mM HEPES (pH 7.5). Reaction rates for SLO and 15-HLO were measured at varying substrate concentrations, 1−60 μM, to reveal the degree of inhibition with increasing amounts of fatty sulfate. All substrates exhibited typical lag phase behavior for both SLO and 15-HLO; therefore, the maximal rate was used as the approximate steady-state rate. Enzymatic reactions were initiated by the addition of ≈3 nM SLO (80 ± 5% Fe) and ≈200 nM 15-HLO (50 ± 5% Fe).

Irreversible Inhibition of 15-HLO by Fatty Sulfates. A sample of 15-HLO (6 μM) was incubated with LS (600 μM) for ≈5 min, dialyzed versus 25 mM HEPES (pH 7.5) for 10 h, and measured for enzyme activity using LA. Control samples that contained no LS were dialyzed in parallel. The dialyzed samples were subsequently passed through a 2 mL SP-Sepharose column (Pharmacia), eluted with 500 mM NaCl, and assayed for activity.

The effect of sequential substrate additions to 15-HLO was measured as follows. An aliquot of 9 μM LS was added to 200 nM 15-HLO and the reaction was allowed to proceed to completion. This was repeated four additional times and the rates were recorded. The effect of sequential enzyme additions to a constant concentration of LS was measured as follows. Increasing amounts of 15-HLO (from 0.1 to 2 mM) were added to a particular concentration of LS until the rate reached ≈0.001 abs_{234}/s. This was done for various LS concentrations (from ≈3 to ≈200 mM), and the amount of 15-HLO needed to achieve ≈0.001 abs_{234}/s was then graphed versus the concentration of LS.

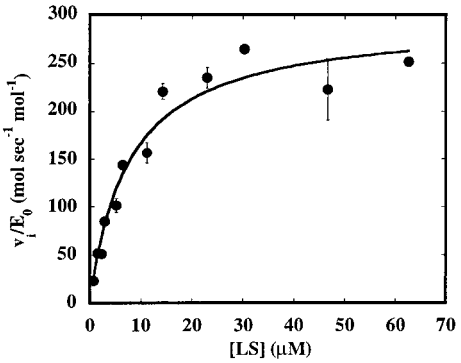

FIGURE 2: Michaelis−Menten kinetics of LS catalysis by SLO in 10 mM CHES (pH 9.2), where $K_m = 7.7 \pm 1.5$ μM and $k_{cat} = 296 \pm 19$ s^{-1}.

Detergent and Ionic Strength. Steady-state kinetics for LS catalysis by 15-HLO were measured in the presence of 50 μM Tween 20R (0.006%, w/v) at varying substrate concentrations, in the specified reaction buffers. Enzymatic rates were also measured in the presence of various other detergents to assess the role of detergent concentration on fatty sulfate aggregation and substrate inhibition. The detergents assayed were Tween 20 (cmc ≈ 0.06 mM), Tween 20R (cmc ≈ 0.06 mM), cholate (cmc ≈ 14 mM), and *n*-heptyl-D-glucopyranoside (cmc ≈ 70 mM). Reaction rates for 15-HLO were measured at ≈60 μM LS using a concentration of ≈10% and ≈80% of the cmc of the specified detergent (25 mM HEPES, pH 7.5). The effect of ionic strength on LS catalysis by 15-HLO was also assayed by running substrate reactions in 25 mM HEPES (pH 7.5) containing 100 and 500 mM NaCl. Control experiments containing no detergent or NaCl were performed in parallel.

RESULTS

Protein Purification. SLO and 15-HLO were purified with yields of ≈4 and ≈50 mg/L and metal contents of 80 ± 5% and 50 ± 5%, respectively (*18*).

Surface Tension Measurements. The cmc's of LA, LS, AS, and diES in the corresponding kinetic buffers were determined. In 25 mM HEPES (pH 7.5), LA had a cmc of 48 ± 11 μM, LS had a cmc of 72 ± 13 μM, and AS had a cmc of 57 ± 5 μM. In 10 mM HEPES (pH 7.5), diES had a cmc of 15 ± 0.7 μM. In 10 mM CHES (pH 9.2), LS had a cmc of 65 ± 10 μM, diES had a cmc of 8 ± 0.4 μM, and AS had a cmc of 80 ± 1.4 μM (*13*).

Steady-State Kinetics of SLO. SLO exhibited hyperbolic steady-state kinetics in 10 mM CHES (pH 9.2) for LS, AS, and diES (Table 1). The steady-state kinetic parameters for LS, K_m and k_{cat}, were determined to be 7.7 ± 1.5 μM and 296 ± 19 s^{-1}, respectively (Figure 2, Table 1). These results are in good agreement with those previously published (*17*).

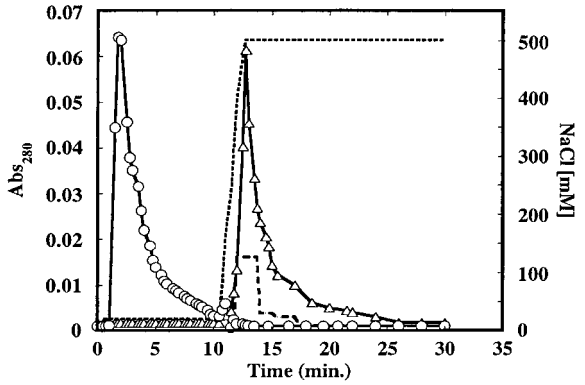

FIGURE 3: SP-Sepharose purification of dialyzed 15-HLO (triangles) and dialyzed LS-treated 15-HLO (circles) in 25 mM HEPES (pH 7.5). All fractions of the LS-treated 15-HLO were devoid of lipoxygenase activity, while the 15-HLO fractions showed greatest activity coincident with the protein elution (dashed). The elution of protein was instigated by a step gradient of 500 mM NaCl (dotted).

Table 1

	K_m (μM)	k_{cat} (s^{-1})	k_{cat}/K_m ($s^{-1}\,\mu M^{-1}$)	K_iK_{aggr} (μM^6)
		SLO (pH 9.2)		
LA	12.4 ± 1.1	276 ± 5	22.3 ± 2.4	- -
LS	7.7 ± 1.5	296 ± 19	38.4 ± 7.9	- -
AS	8.6 ± 1.3	352 ± 17	40.9 ± 6.5	- -
diES	4.5 ± 0.6	289 ± 11	64.2 ± 8.9	- -
LS (pH 7.5)	10.5 ± 4.7	360 ± 60	34.3 ± 16.4	
		15-HLO (pH 7.5, $n = 6$)		
LA	5.5 ± 1.0	9.4 ± 0.6	1.7 ± 0.3	- -
LS	4.0 ± 0.7	6.7 ± 1.4	1.7 ± 0.2	$2.0 \times 10^7 \pm 3.0 \times 10^6$
AS	2.9 ± 0.5	4.5 ± 0.9	1.6 ± 0.2	$1.2 \times 10^8 \pm 2.0 \times 10^7$
diES	12.8 ± 2.8	13.1 ± 3	1.0 ± 0.1	$8.9 \times 10^5 \pm 7.2 \times 10^4$
		15-HLO W/Detergent ($n = 2$)		
LS	23 ± 16	12.3 ± 8.8	0.54 ± 0.1	$513 \pm 102\ \mu M^2$

The kinetic parameters for LA, AS, and diES are also listed in Table 1 and no substrate inhibition was detected. The structures of the fatty sulfates are shown in Figure 1.

Irreversible Inhibition of 15-HLO by Fatty Sulfates. The fatty sulfates were substrates for 15-HLO at low concentration (less than $\approx$15 μM), but at higher concentration (greater than $\approx$15 μM) they were inhibitors. This inhibition was determined to be irreversible through the following experiments. First, a sample of 15-HLO (6 μM) and LS (600 μM) was dialyzed against 25 mM HEPES (pH 7.5), containing 50 μM Tween 20, for 10 h, and no activity was recovered. A parallel sample of untreated 15-HLO was also dialyzed, and greater than 90% activity was recovered. Second, these same dialyzed samples were then passed through an SP-Sepharose column (cation exchange). The control 15-HLO sample, which had no LS added, bound to the SP-Sepharose column and retained activity after being eluted with a 500 mM NaCl wash (Figure 3). The LS-treated 15-HLO did not bind to the column and it remained inactive (Figure 3). This result suggested that multiple negatively charged LS molecules bound to lipoxygenase, and this binding affected the retention on the SP-Sepharose column. Third, the addition of increasing amounts of 15-HLO to a solution of 70 μM LS overcame the inhibition by LS at approximately 0.9 μM 15-HLO. This indicated consumption of the inhibitory species by 15-HLO (i.e., through irreversible activation, as described by Segel) and that the excess amount of 15-HLO

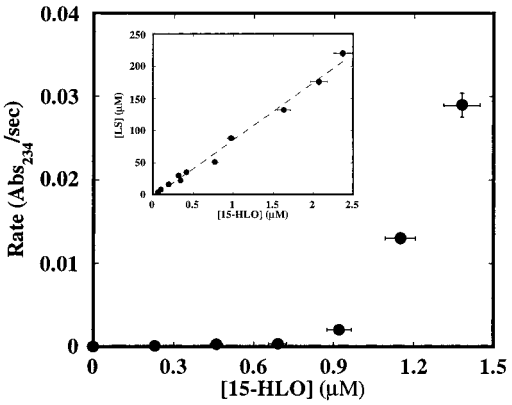

FIGURE 4: 15-HLO concentration is plotted versus its corresponding rate at $\approx$70 μM LS in 25 mM HEPES (pH 7.5). LS inhibition was considered overcome when the rate became greater than 0.001 abs_{234}/s. The 15-HLO concentration required to overcome inhibition is plotted versus the initial concentration of LS (inset). A linear fit to the data yielded the equation $[LS] = -4 + 89[15\text{-HLO}]$, where $\approx$1.2 μM 15-HLO is required to overcome the inhibition of 100 μM LS ($R^2 = 0.99$).

was responsible for converting the remaining substrate to product (Figure 4) (*20*). The amount of enzyme required to overcome the inhibition (i.e., a rate of $\approx$0.001 abs_{234}/s) increased linearly with increasing LS concentration (Figure 4, inset). The fit to this line ($[LS] = -4 + 89[15\text{-HLO}]$) indicated that at 100 μM LS, $\approx$1.2 μM 15-HLO is required to achieve a rate of 0.001 abs_{234}/s. To prove that this effect was not due to a synthetic impurity, LS (9 μM) was added to a solution of 15-HLO (200 nM) and was allowed to proceed to complete conversion to product. At this point, an additional aliquot of 9 μM LS was added and the rates were recorded. This was repeated a total of five times, and after the final addition of 9 μM LS (45 μM total) a significant amount of activity remained (45% of the activity of the first 9 μM addition). This was markedly greater than the rate after one addition of 45 μM LS (0.05% of the activity of the first 9 μM LS addition). This result indicated that the inhibition was dependent on the initial concentration of LS and not the total amount of LS added, suggesting a fatty sulfate aggregate and not a synthetic byproduct as the inhibitory species. The loss of the activity observed after the fifth LS addition, relative to the first addition (45% the initial activity), was due to the well-documented auto-inactivation of 15-HLO and was not attributed to the aggregate inhibition (*21*).

Steady-State Kinetics of 15-HLO. 15-HLO exhibited a striking parabolic inhibitory response to increasing amounts of LS in 25 mM HEPES (pH 7.5) (Figure 5). 15-HLO (200 nM) reached a maximum rate of $\approx$5 mol of LS consumed per second per mole of enzyme (mol s^{-1} mol^{-1}) at $\approx$12 μM LS, while at concentrations above $\approx$55 μM LS the rate was negligible. The parabolic shape of the rate curve was indicative of substrate inhibition due to the presence of a secondary binding site that inhibits catalysis. The simple monomer binding site model which forms a nonproductive complex (Scheme 1, eq 1) yielded a poor fit to the data and a negative K_m value, indicating an incorrect model. Inclusion of a catalytically competent allosteric complex (eq 2), as seen for the OS inhibition of SLO, did not improve the fit (*13*). Sequential binding of two LS molecules to form a nonproductive complex (eq 3), as proposed for SLO by Wang et

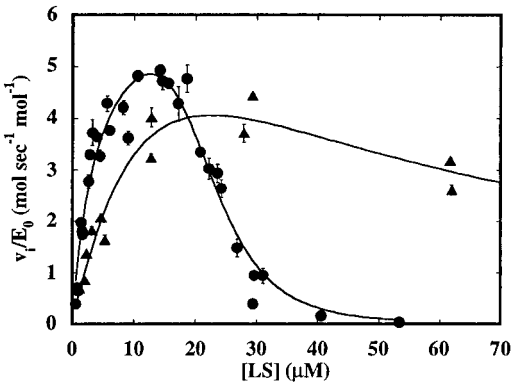

FIGURE 5: Steady-state inhibition kinetics of LS catalysis by 15-HLO (200 nM) in 25 mM HEPES (pH 7.5) (solid circles). The data are fitted to eq 7, Scheme 2, where $K_m = 4.0 \pm 0.7$ μM, $k_{cat}/K_m = 1.7 \pm 0.2$ μM^{-1} s^{-1}, $K_iK_{aggr} = 2.0 \times 10^7 \pm 3.0 \times 10^6$ μM^6, and $n = 6$ [$R^2 = 0.94$, RMS = 1.3]. The effect of 50 μM Tween 20R on the steady-state kinetics of LS catalysis by 15-HLO in 25 mM HEPES (pH 7.5) (solid triangles). The data are fitted to eq 7, where $K_m = 23 \pm 16$ μM, $k_{cat}/K_m = 0.54 \pm 0.1$ μM^{-1} s^{-1}, $K_iK_{aggr} = 513 \pm 102$ μM^2, and $n = 2$ [$R^2 = 0.92$, RMS = 1.2]. The units of the graph are moles of substrate consumed per second per mole of enzyme (mol s^{-1} mol^{-1}).

Scheme 1

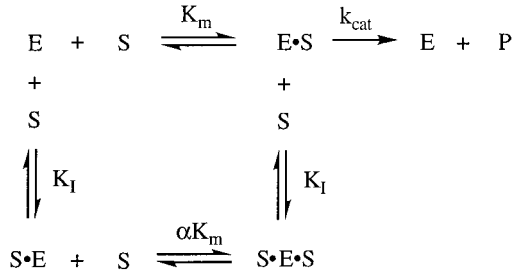

$$v = k_{cat}/K_m[S]/(1 + (1/K_m + 1/K_i)[S] + 1/\alpha K_mK_i[S]^2) \quad (1)$$

$$v = (k_{cat}/K_m[S] + (\beta k_{cat}/\alpha K_mK_i))/(1 + (1/K_m + 1/K_i)[S] + 1/\alpha K_mK_i[S]^2) \quad (2)$$

$$v = k_{cat}/K_m[S]/(1 + (1/K_m + 1/K_i)[S] + (1/K_m\alpha K_i + 1/K_iK_{ii})[S]^2 + 1/K_m\alpha K_i\delta K_{ii}[S]^3) \quad (3)$$

al. (*12*), yielded a good fit to the data but required negative fit parameters, indicating a poor model (fit not shown). The data were best fit by the formation of a fatty sulfate aggregate, prior to enzyme binding, that inhibits catalysis by yielding a nonproductive aggregate−enzyme complex (Scheme 2, Figure 5). The formation of the substrate aggregate (eqs 4 and 5) was required to incorporate a higher power substrate concentration term ($[S]^n$) into the rate equation (eq 6) and to achieve a good mathematical fit to the steep decline in activity (eq 7, Figure 5). Inclusion of an irreversible step after aggregate binding (eq 8) did fit the data but yielded negative fit values. This suggested that the substrate aggregate bound extremely tightly to the protein (K_i) which may mask an irreversible chemical step after aggregate binding. This corroborated the dialysis and cation exchange experiments, which showed the LS molecules tightly bound to 15-HLO. From Scheme 2, eqs 4−7 were derived which allowed for the determination of four parameters: k_{cat}/K_m, K_m, K_iK_{aggr}, and n, where n is the approximate value for the number of molecules in the aggregate. The steady-state parameters, k_{cat}/K_m and k_{cat}, have the standard definitions, while the combined term of K_iK_{aggr} can be considered an indirect measure of enzyme inhibition. It contains both the propensity of aggregate formation (K_{aggr}) and the dissociation constant of inhibitor aggregate binding to the enzyme (K_i). The K_iK_{aggr} term has an inverse relationship to the magnitude of inhibition; hence, a lower value of K_iK_{aggr} indicates stronger inhibition by the fatty sulfate aggregate. The approximate aggregate size, n, was determined by comparisons of the quality of fits with different integer values of n, and its error was determined by approximation.

Scheme 2

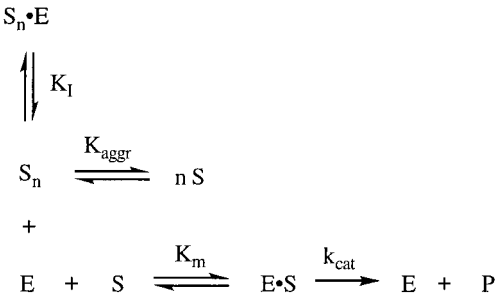

$$K_{aggr} = K_D{}^1K_D{}^2K_D{}^3\cdots K_Dn^{-1} \quad (4)$$

$$[S_n] = [S]^n/K_{aggr} \quad (5)$$

$$v = k_{cat}/K_m[S]/(1 + 1/K_m[S] + 1/K_i[S_n]) \quad (6)$$

$$v = k_{cat}/K_m[S]/(1 + 1/K_m[S] + 1/K_iK_{aggr}[S]^n) \quad (7)$$

$$v = k_{cat}/K_m[S]/(1 + 1/K_m[S] + 1/K_iK_{aggr}[S]^n + k_{irrev}/K_iK_{aggr}[S]^n) \quad (8)$$

The best fit to the LS rate curves for 15-HLO (eq 7) yielded the kinetic parameters listed in Table 1 and displayed in Figure 5. 15-HLO was also inhibited by AS (25 mM HEPES, pH 7.5), with a maximal rate of ≈4 mol s^{-1} mol^{-1} at ≈15 μM AS (Figure 6), and was fit to eq 7 (Table 1). DiES inhibited 15-HLO (10 mM HEPES, pH 7.5), with a maximal rate of ≈4 mol s^{-1} mol^{-1} at ≈8 μM diES (Figure 6), and could be best fit to eq 7 with a diES aggregate of $n = 6 \pm 2$ (Table 1). This is in contrast to the saturation kinetics results for 15-HLO with LA, in which no substrate inhibition is observed (Table 1).

Under the same pH conditions as in the 15-HLO reactions (25 mM HEPES, pH 7.5), SLO exhibited saturation kinetics with LS yielding a K_m of 10.5 ± 4.7 μM and a k_{cat} of 360 ± 60 s^{-1} (Table 1). This experiment demonstrated that the solution-state aggregates that inhibit 15-HLO did not significantly affect SLO catalysis, though a slight deviation from the steady-state fit may suggest slight monomer inhibition.

Detergent Effect on Catalysis. The steady-state kinetics of 15-HLO with LS were studied in the presence of 50 μM Tween 20R in order to assess the role of substrate aggregates as inhibitors. Immediate addition of Tween 20R (50 μM) to an inhibited mixture of 200 nM 15-HLO and 50 μM LS did not recover activity. However, if the detergent was added to

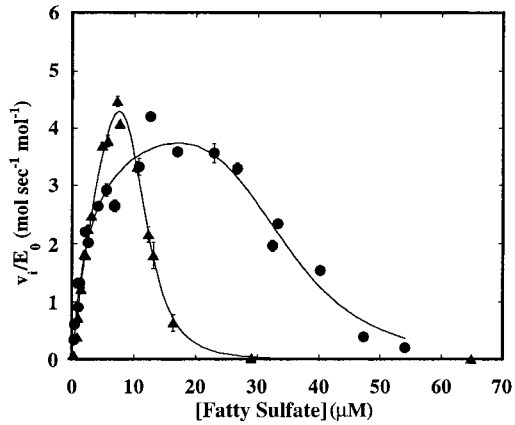

FIGURE 6: Steady-state inhibition kinetics of AS catalysis by 15-HLO in 25 mM HEPES (pH 7.5) (solid circles). The data are fitted to eq 7, where $K_m = 2.9 \pm 0.5$ μM, $k_{cat}/K_m = 1.6 \pm 0.2$ μM^{-1} s^{-1}, $K_iK_{aggr} = 1.2 \times 10^8 \pm 2.0 \times 10^7$ μM^6, and $n = 6$ [$R^2 = 0.96$, RMS = 0.87]. Steady-state inhibition kinetics of diES catalysis by 15-HLO in 10 mM HEPES (pH 7.5) (solid triangles). The data are fitted to eq 7, where $K_m = 12.8 \pm 2.8$ μM, $k_{cat}/K_m = 1.0 \pm 0.1$ μM^{-1} s^{-1}, $K_iK_{aggr} = 8.9 \times 10^5 \pm 7.2 \times 10^4$ μM^6, and $n = 6$ [$R^2 = 0.99$, RMS = 0.53].

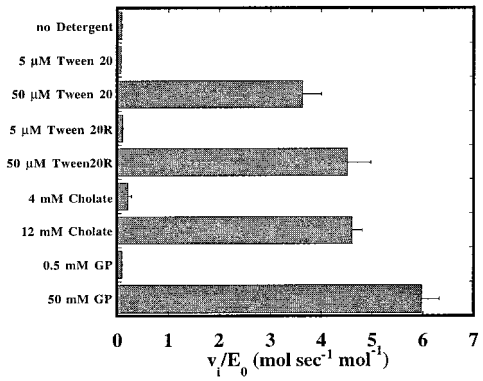

FIGURE 7: Effect of detergent concentration on LS catalysis by 15-HLO. Substrate concentration is ≈60 μM LS, and reactions were run in 25 mM HEPES (pH 7.5).

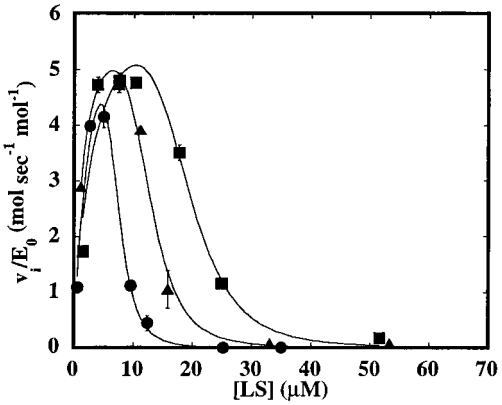

FIGURE 8: Effect of ionic strength on the steady-state kinetics of LS catalysis by 15-HLO in 25 mM HEPES (pH 7.5). Enzymatic rates were measured at increasing amounts of sodium chloride: 0 mM NaCl (squares), 100 mM NaCl (triangles), 500 mM NaCl (circles). The data are fitted with eq 7 yielding K_iK_{aggr} values of $6.0 \times 10^6 \pm 2.5 \times 10^6$, $3.5 \times 10^5 \pm 7.5 \times 10^4$, and $3.9 \times 10^4 \pm 8.2 \times 10^3$ μM^6, respectively.

the fatty acid solution prior to addition of the enzyme, activity was observed. The addition of detergent reduced the extreme parabolic substrate inhibition to a slight parabola, indicating only minimal inhibition by LS (Figure 5). The rate data could be fit using the aggregate inhibitor model (eq 7, Scheme 2), however, the n is reduced to 2 ($K_m = 23 \pm 16$ μM, $k_{cat}/K_m = 0.54 \pm 0.1$ μM^{-1} s^{-1}, $K_iK_{aggr} = 513 \pm 102$ μM^2, $n = 2$, Table 1). The data could also be fit with the monomer LS binding to the allosteric site, forming a noncatalytic species (eq 1, Scheme 1) ($k_{cat}/K_m = 0.54 \pm 0.1$, $(1/K_m + 1/K_i) = 0.044 \pm 0.3$, $1/\alpha K_mK_i = 0.002 \pm 0.0004$). This fit did not require an aggregate formation and was simply due to the monomer binding to an unproductive allosteric site. Kinetic models utilizing either a catalytically competent allosteric complex (eq 2) or multiple allosteric sites (eq 3) yielded negative fit parameters and were considered inaccurate models.

The "rescue" of activity by the detergent was not dependent on the detergent charge and/or structure but was only observed when the detergent was close to its cmc value. At ≈60 μM LS, 15-HLO (200 nM) exhibited a negligible rate in 25 mM HEPES (pH 7.5), however, at detergent concentrations of ≈75% of their respective cmc values (Tween 20, Tween 20R, cholate, and *n*-heptyl-D-glucopyranoside), the rate of 15-HLO increased by ≈2000−3000% (Figure 7). At concentrations of ≈10% of their cmc values, these detergents yielded no significant effect on the enzymatic rate of 15-HLO (Figure 7), indicating that catalysis was dependent on the presence of detergent micelles, and not on the particular detergent structure and/or charge.

The NaCl concentration of the LS substrate solutions was also varied in order to address the role of fatty sulfate aggregation on 15-HLO catalysis since higher ionic strength increases aggregation (*22*). The changes in the maximum rate of 15-HLO upon increasing amounts of LS were measured at 100 and 500 mM NaCl in 25 mM HEPES (pH 7.5) (Figure 8). Fits to the data with eq 7 yielded a steady decrease in K_iK_{aggr} values from 6.0×10^6 μM^6 (0 mM NaCl) to 3.5×10^5 μM^6 (100 mM NaCl) and 3.9×10^4 μM^6 (500 mM NaCl), indicating increased inhibition. This was qualitatively seen by the decrease in the amount of LS required to completely inhibit 15-HLO and suggested that the higher ionic strength increases the concentration of the substrate aggregate.

DISCUSSION

Recently, inhibition of SLO and 15-HLO by OS has been shown to proceed through an allosteric binding site which modulates substrate turnover by changing the microscopic rate constants of catalysis (*13*). The K_i of OS for SLO (≈0.6 μM) is markedly lower than that of OA ($K_i \approx 20$ μM), presumably due to an increase in the ionic strength of the sulfate moiety (*13*). In the current study, we have extended this investigation of the effect of the sulfate moiety on lipoxygenase function by synthesizing several fatty sulfate substrates (LS, AS, diES) and assaying their catalytic and inhibitory properties on SLO and 15-HLO.

The steady-state parameters of fatty sulfate catalysis by SLO indicate that the sulfate moiety of the substrate increases the relative k_{cat}/K_m as compared to those for the natural carboxylic acid substrate, LA (Figure 2, Table 1). The k_{cat}/K_m for LS is ≈1.7-fold greater than that of LA, while its k_{cat} is approximately the same as that of LA. AS displays a $k_{cat}/$

K_m value similar to that of LS, but diES is catalyzed with an even greater efficiency than either LS or AS. In contrast, the k_{cat} for diES is within experimental error of that of LS, but both are ~1.2-fold lower than that of AS. These data indicate that SLO has an optimal rate of substrate capture (k_{cat}/K_m) for diES yet an optimal rate of product release (k_{cat}) for AS.

The fatty sulfates do not inhibit SLO which indicates a markedly different behavior than displayed by the natural substrate, LA. Previously, Wang et al. observed that LA inhibits SLO at high concentrations (≈60 μM, pH 10) (*12*). This is consistent with other investigations, which demonstrated an increase in the KIE with increasing LA concentration for both SLO and 15-HLO (*14, 15*). These studies indicate that LA binds to the allosteric site on both SLO and 15-HLO, albeit with a much lower affinity than that of OS (LA, $K_D > 50$ μM, OS, $K_D \approx 0.6$ μM, SLO). The diene-containing fatty sulfates (LS, AS, diES), however, are not inhibitors to SLO and exhibit saturation steady-state kinetics at pH 9.2; this indicates that the diene-containing fatty sulfates bind preferentially to the catalytic site and not significantly to the allosteric site of SLO. This is the opposite of the binding preference of the fatty sulfate inhibitor, OS, which binds preferentially to the allosteric site and indicates a structural selectivity between the catalytic and allosteric sites of SLO. The two fatty sulfates, OS and LS, have the same carbon chain length and charge; therefore, the selectivity of binding is due to the difference in the degree of unsaturation between the two molecules (OS,C_{18}:Δ1 and LS, C_{18}:Δ2). This binding selectivity between LS and OS could be due to either a conformational difference between the monoene- and diene-containing fatty sulfates and/or a $\pi-\pi$ stacking of the diene moiety with an aromatic residue within the catalytic site (*21*). In either case, SLO manifests a selectivity between the two molecules which is remarkable considering the structural similarity between LS and OS.

The fatty sulfates (LS, diES, AS) are substrates for 15-HLO as well; however, the catalytic selectivity is slightly different from that of SLO. The steady-state parameter of k_{cat}/K_m for 15-HLO, determined using eq 7, indicates that LS and AS are both catalyzed to approximately the same efficiency as that of LA (Table 1). However, all three manifest k_{cat}/K_m values that are ≈1.6-fold greater than that of diES. The k_{cat} for diES, in contrast, is ≈2-fold greater than that of LS, ≈3-fold greater than that of AS, and ≈1.4-fold greater than that of LA. These trends in kinetic parameters indicate that the rate of substrate capture (k_{cat}/K_m) for 15-HLO is best for LA, LS, and AS, while the rate of product release (k_{cat}) is best for diES. This is a different trend from that of SLO, which suggests that the active sites of 15-HLO and SLO contain slightly different binding determinants. This is within reason, since both enzymes utilize different substrates in vivo (15-HLO, AA; SLO, LA) and have different active site cavities (*23, 24*). It is interesting to note that both SLO and 15-HLO are capable of catalyzing a fatty sulfate substrate (AS, C_{20}:Δ4) that is four atoms longer on the anionic side of the 1,4-diene than LA (C_{18}:Δ2). This suggests that the charge stabilization epitope for both SLO and 15-HLO is remarkably flexible and can accommodate the additional four-atom length of AS (two additional carbons, a sulfur, and an oxygen). For 15-HLO, Lys_{403} has been proposed as the cation that interacts with the substrate anion; however, it is unclear how it could accommodate both AS and LA considering their chain length difference (*21*). Additional cationic residues could possibly stabilize the anion depending on the particular substrate; we are currently investigating these questions through mutagenesis.

At high concentration, however, the fatty sulfates are potent inhibitors to 15-HLO, as illustrated by the striking parabolic response of 15-HLO to increasing amounts of substrate (Figure 5). The inhibition is irreversible, as illustrated by the lack of enzyme activity recovered after dialysis. In addition, the dialyzed LS-treated 15-HLO does not bind to a cation exchange column, unlike native 15-HLO, which indicates that the protein has an increased overall negative charge (Figure 3). This is most likely due to the adhesion of multiple LS molecules to 15-HLO, which adds negative charge to the protein, thus repelling it from the cation exchange column. These LS molecules cannot be dialyzed away, and are either bound extremely tightly to the protein or covalently attached. The inhibition of 15-HLO by LS, however, can be overcome by the addition of excess 15-HLO (Figure 4). The amount of excess 15-HLO needed to overcome the inhibition increases linearly with substrate concentration and is determined to be ≈1.2% of the total substrate concentration (Figure 4, inset). It is unclear why the relationship is linear, but the simplest explanation is that the concentration of the inhibitor increases linearly with LS concentration; further studies are required. The observed inhibition is not due to a trace synthetic impurity since sequential additions of LS (up to 45 μM LS total) yield high activity, as compared to the complete inhibition with only one addition of 45 μM LS. This indicates that inhibition is dependent on the initial LS concentration and not the total amount of LS added, which points to the presence of a substrate aggregate as the inhibitory species of 15-HLO.

This hypothesis of aggregate inhibition for 15-HLO is supported by the fact that detergent (at cmc concentration) significantly reduces the substrate inhibition of 15-HLO when it is added to the substrate prior to enzyme addition (Figure 7). This "rescue" of activity by detergent is most likely due to a breakup of the inhibitory substrate aggregates by formation of mixed micelles between the fatty sulfate and detergent. These mixed micelles are no longer inhibitory, and the fatty sulfate can then be catalyzed through micelle surface kinetics (Figure 5) (*25*). The resultant rate curves of 15-HLO with detergent present could be fit with either a dimer aggregate ($n = 2$, eq 7) or a monomer binding to the allosteric site (Scheme 1, eq 1); however, we cannot differentiate between these two inhibition mechanisms at this time. The presence of a substrate aggregate is further supported by the increase in inhibition as ionic strength increases, i.e., NaCl concentration, a known inducer of lipid aggregation (*22*). The increase in salt concentration decreases the amount of LS needed to fully inhibit 15-HLO, as seen by their lowered K_iK_{aggr} values (Figure 8). It should be noted that millimolar concentrations of SDS do not inhibit 15-HLO, so we believe the inhibition is not due to a detergent effect; however, further studies are needed. Taken together, these data indicate that 15-HLO is inhibited by an aggregate of fatty sulfate substrates.

This conclusion is critical to the analysis of the enzymatic rate data for 15-HLO, since the rate data cannot be fit with

a simple monomer allosteric binding site model (Scheme 1, eq 1) nor sequential binding of two substrate molecules to an allosteric site (eq 3). The steep parabolic inhibition, however, can be mathematically fit with the inclusion of an aggregate binding site into the kinetic inhibition model for 15-HLO (Scheme 2, eq 7, Figure 5). Scheme 2 assumes that the inhibitory fatty sulfate aggregate forms prior to enzyme interaction (K_{aggr}) and subsequently binds to the protein (K_i). Based on this kinetic model, the fit parameters indicate that diES is a more potent inhibitor to 15-HLO than either LS or AS. The inhibition (K_iK_{aggr}) by diES is ≈22-fold greater than that by LS, and ≈135-fold greater than that by AS [diES > LS > AS] (Table 1). This inhibition trend roughly correlates with the cmc of each substrate, since the value for diES (15 ± 1 μM) is 4−5 times lower than the cmc of both LS (72 ± 13 μM) and AS (57 ± 5 μM), which supports a dependence of fatty sulfate aggregation on 15-HLO inhibition. The cmc values, however, do not fully explain the differences in K_iK_{aggr}, since LS inhibition is ≈6-fold greater than that of AS, even though its cmc value is higher than that of AS. This suggests that the chemical structure of the fatty sulfate may also play a role in aggregate binding and the inactivation of 15-HLO.

In conclusion, conversion of fatty acid substrates to their corresponding fatty sulfates renders suitable substrates for SLO which do not bind to the allosteric site and inhibit the enzyme. This indicates a selectivity of OS binding to the allosteric site over that of LS, presumably due to the change in bond saturation. The fatty sulfates, however, are potent inhibitors to 15-HLO which irreversibly abolish activity above ≈50 μM. This inhibition is due to the presence of fatty sulfate aggregates, which denature and/or covalently modify the protein, rendering it inactive. In contrast, aggregates of LA do not significantly inhibit 15-HLO, though the cmc of LA is ≈2-fold lower than that of LS. This suggests that the sulfate moiety plays a critical role in aggregate binding, suggesting the presence of a polycationic binding site on 15-HLO. This result may have broader significance, since Gillmor et al. have proposed the presence of a membrane docking site on the β-barrel domain of rabbit 15-lipoxygenase which may be structurally related to the aggregate binding site proposed in this study (*23*). We are currently investigating this hypothesis with EI-MS and site-directed mutagenesis in order to ascertain the location of the aggregate binding site and its mechanism of lipid binding.

ACKNOWLEDGMENT

The authors thank Prof. D. Deamer for the use of the Cahn electromicrobalance and helpful comments. Additional thanks goes to the Holman research group for technical support.

REFERENCES

1. Samuelsson, B., Dahlen, S. E., Lindgren, J. A., Rouzer, C. A., and Serhan, C. N. (1987) *Science 237*, 1171−1176.
2. Sigal, E. (1991) *J. Am. Phys. Soc. 260*, 13−28.
3. Steele, V. E., Holmes, C. A., Hawk, E. T., Kopelovich, L., Lubet, R. A., Crowell, J. A., Sigman, C. C., and Kelloff, G. J. (1999) *Cancer Epidemiol., Biomarkers Prev. 8*, 467−483.
4. Gosh, J., and Myers, C. E. (1998) *Proc. Natl. Acad. Sci. 95*, 13182−13187.
5. Harats, D., Shaish, A., George, J., Mulkins, M., Kurihara, H., Levkovitz, H., and Sigal, E. (2000) *Arterioscler. Thromb., Vasc. Biol. 20*, 2100−2105.
6. DeGroot, J. J. M. C., Aasa, R., Malmstrom, B. G., Slappendel, S., Veldink, G. A., and Vliegenthart, J. F. G. (1975) *Biochim. Biophys. Acta 377*, 71−79.
7. Solomon, E. I., Zhou, J., Neese, F., and Pavel, E. G. (1997) *Chem. Biol. 4*, 795−808.
8. Gardner, H. W. (1989) *Biochim. Biophys. Acta 1001*, 274−281.
9. Glickman, M. H., and Klinman, J. P. (1995) *Biochemistry 34*, 14077−14092.
10. Glickman, M. H., and Klinman, J. P. (1996) *Biochemistry 35*, 12882−12892.
11. Hwang, C. C., and Grissom, C. B. (1994) *J. Am. Chem. Soc. 116*, 795−796.
12. Wang, Z. X., Killilea, S. D., and Srivastava, D. K. (1993) *Biochemistry 32*, 1500−1509.
13. Mogul, R., Johansen, E., and Holman, T. (2000) *Biochemistry 39*, 4801−4807.
14. Glickman, M. H., Wiseman, J. S., and Klinman, J. P. (1994) *J. Am. Chem. Soc. 116*, 793−794.
15. Lewis, E. R., Johansen, E., and Holman, T. R. (1999) *J. Am. Chem. Soc. 121*, 1395−1396.
16. Sailer, E. R., Schweizer, S., Boden, S. E., Ammon, H. P. T., and Safayhi, H. (1998) *Eur. J. Biochem. 256*, 364−368.
17. Bild, G. S., Ramadoss, C. S., and Axelrod, B. (1977) *Lipids 12*, 732−735.
18. Holman, T. R., Zhou, J., and Solomon, E. I. (1998) *J. Am. Chem. Soc. 120*, 12564−12572.
19. Verhagen, J., Vliegenthart, J. F. G., and Boldingh, J. (1978) *Chem. Phys. Lipids 22*, 255−259.
20. Segel, I. H. (1975) *Enzyme Kinetics*, John Wiley and Sons, Inc., New York, NY
21. Gan, Q.-F., Browner, M. F., Sloane, D. L., and Sigal, E. (1996) *J. Biol. Chem. 271*, 25412−25418.
22. Tanford, C. (1980) *The Hydrophobic Effect*, John Wiley and Sons, Inc., New York, NY
23. Gillmor, S. A., Villasenor, A., Fletterick, R., Sigal, E., and Browner, M. (1997) *Nat. Struct. Biol. 4*, 1003−1009.
24. Minor, W., Steczko, J., Boguslaw, S., Otwinowski, Z., Bolin, J. T., Walter, R., and Axelrod, B. (1996) *Biochemistry 35*, 10687−10701.
25. Carman, G. M., Deems, R. A., and Dennis, E. A. (1995) *J. Biol. Chem. 270*, 18711−18714.

BI002581A